Multiple pathways of capillary permeability.

E M Renkin

Circ Res. 1977;41:735-743
doi: 10.1161/01.RES.41.6.735
Circulation Research is published by the American Heart Association, 7272 Greenville Avenue, Dallas, TX 75231

Print ISSN: 0009-7330. Online ISSN: 1524-4571

Circulation Research DECEMBER 1977
VOL. 41 NO. 6
An Official Journal of the American Heart Association

BRIEF REVIEWS

Multiple Pathways of Capillary Permeability

EUGENE M. RENKIN

THIS IS A REVIEW of our current understanding of capillary permeability and its relation to endothelial morphology. It is based partly on material gathered for a chapter on capillary endothelia in a handbook on epithelial transport mechanisms.[1] For more general reviews of transcapillary exchange, the reader is referred to the appropriate chapters in the *Handbook of Physiology*,[2-4] and to the chapter by C.C. Michel in Bergel's *Cardiovascular Fluid Dynamics*.[5] The special case of renal glomerular capillary permeability is considered by separate reviews.[6, 7]

Morphological Identification of Transport Pathways

The capillary endothelium of most vertebrate tissues and organs consists of a single layer of flattened cells bound together within an acellular basal lamina, presumably secreted by the cells. Materials may penetrate this structure by passing directly through the cells, that is through two thicknesses of cell membrane and a layer of cytoplasm, or they may penetrate without entering the cells, by extracellular channels through them, or through the junctions between them. Figure 1 is a diagram of various capillary transport pathways.

Light microscopy has been used to study permeability of exposed mesenteric capillaries (nonfenestrated) of amphibians and mammals to dyes and fluorescent tracers. Though resolution is insufficient to identify transport pathways on the scale of Figure 1, this method provides valuable information about overall patterns of solute transport along individual capillaries and in specific parts of the microvascular network. Small dye molecules (not bound to plasma proteins) appear to cross the walls of capillaries of the frog's mesentery unevenly. During the first few seconds of perfusion, patterns of increased density appear outside the capillaries at intervals of 27–30 μm. These correspond closely to the separation of intercellular junctions. Superimposed on this pattern are larger scale inhomogeneities, substantial regions of the capillaries allowing more dye penetration than others. Protein-bound dyes or other dye-labeled macromolecules also show these large scale inhomogeneities, appearing in highest concentrations in localized regions near the junctions of venous capillaries.[19-21] The number of such "leaky" areas is increased in capillary injury, and they may then extend to the arterial side of the network. The "leaks" are often considered to represent the large pore pathway of Figure 1 (A-5 and B-5), though the resolution of light microscopy is too low to prove that they occur in junctional areas, or to exclude the possibility of leaks through vesicular chains (Fig. 1, A-6 and B-6).

Florey[22] attempted to demonstrate endothelial pathways for ferrocyanide ions in capillaries of the dog's intestine by deposition of prussian blue, followed by light microscopic examination. Although ferrocyanide is excluded from most cells, he reported the appearance of precipitate within endothelial cell cytoplasm and concluded that transport of small ions was through the cells. Later workers usually consider his result inconclusive, due to limitations of preparation and resolution. Casley-Smith[23] used the same approach with electron micrography to demonstrate exclusively junctional pathways for ferrocyanide and sulfate ions in cerebral and retinal capillaries of rabbits. The most substantial body of work on morphological identification of capillary transport pathways is based on much larger tracer substances.

NONFENESTRATED CAPILLARIES

Simionescu et al.[17, 24] studied distribution of myoglobin (effective molecular radius, a_e = 17 Å)* and two microperoxidases ($a_e \cong 10$ Å) within the endothelium of rat skeletal muscle capillaries after intravascular injection. All three molecules appeared to be excluded from the narrow part of the intercellular junctions, but did appear within cytoplasmic vesicles. Within 30 seconds of administration, the vesicles on the internal (lumenal) surfaces of the endothelial cells were labeled; by 60 seconds, the labels were distributed uniformly in internal and external surface vesicles. Passage was concluded to proceed entirely via the vesicles, either singly or through openings

From the Department of Human Physiology, The University of California, Davis, California.

Original work in this review was supported by U.S. Public Health Service Grants HL 18010 and HL 17998.

Address for reprints: Eugene M. Renkin, Ph.D., Department of Human Physiology, School of Medicine, University of California, Davis, California 95616.

* Stokes-Einstein radius, the radius of a hydrodynamically equivalent sphere. $a_e = RT/6\pi\eta DN$ where R = gas constant, T = absolute temperature, π = 3.14 . . . η = viscosity of medium, D = free diffusion coefficient of the solute in the medium at temperature T, and N = Avogadro's number.[2]

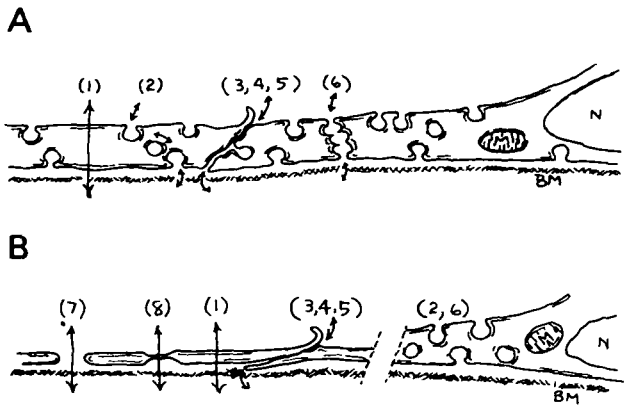

FIGURE 1 *Diagram of transport pathways in capillary endothelium. Panel A: Unfenestrated capillaries (A1α, Bennett et al.[8]), found in skin, skeletal muscle, frog mesentery, intestinal smooth muscle, heart, and lung. Panel B: Fenestrated capillaries (A2α) found in intestinal mucosa, renal cortex (glomerular, peritubular capillaries), and in many glandular organs. The fenestrations are present only in the thin part of the endothelial cell (30–40 nM) which comprises 2–30% of its total surface. The rest of the cell shows all the structures characteristic of A1α capillaries. Many[9] or all[10] of the fenestrae appear to be closed by thin diaphragms. In both sketches, the lumen is at the top, and the basement membrane (BM) is indicated by stippling. N = nucleus; M = a mitochrondrion, just to show that these are present. Presumed transport pathways are as follows. (1) Cellular, directly through endothelial cell membranes and cytoplasm (water, small nonpolar solutes, lipid-soluble solutes). (2) Vesicular, small cytoplasmic vesicles believed to shuttle back and forth between opposing cell surfaces and to exchange fluid and solutes by equilibrating contents at each surface.[11, 12] Though all components of plasma and interstitial fluid except those too large to enter the vesicles may be exchanged, this pathway may be quantitatively significant only for plasma proteins and other large molecules.[13] Macropinocytosis may also contribute to endothelial transport of macromolecules. (3) Lateral diffusion in cell membranes through junctional complexes may provide a pathway for water-insoluble lipids.[14] (4) Narrow, "small pore" junctions may provide pathways for diffusion and ultrafiltration exchange of water and lipid-insoluble solutes up to the size of small plasma proteins. (5) Wide, "large pore" or "leak" junctions permit exchange of plasma proteins and other large molecules as well. The structure of the junctions appears to vary, not only between different tissues and organs, but from arterial to venous regions of the microvascular bed in the same organ.[15, 16] (6) Transitory open channels formed by the confluence of chains of micropinocytotic vesicles may provide an additional extracellular transport pathway. Depending on the size of the vesicular junctions, its characteristics might resemble either the "small pore" or "large pore" pathway.[17] (7) Open fenestrae (without diaphragms) provide a minimally restrictive pathway through the endothelium. (8) The transport function of closed fenestrae depends on the permeability of the diaphragm. It is not certain whether they represent a refinement of the cell membrane pathway (1), an extension of the "small pore" pathway (4), or a specialization of the cell membrane. Simionescu et al.[18] noted that the presence of diaphragms in individual fenestrae intestinal capillaries did not appear to prevent transport of ferritin, dextran, or glycogen particles 100 to 300 Å in diameter. The permeability of the basement membrane may be a significant factor in determining transport rates through the less restrictive pathways enumerated. Not included in this figure are the "open" capillaries or sinusoids of the liver and spleen (B3α) and the "tight junction" capillaries of the brain (A1β).*

formed by chains of vesicles. Horseradish peroxidase (a_e = 25 Å) and ferritin (55 Å) are also reported to appear rapidly in cytoplasmic vesicles on the luminal surface following injection, with subsequent extension to the external surface within 1 minute.[25, 26] The former also penetrates into the intercellular junctions, but it is difficult to be sure whether this is a primary transit route or if the external labeling of the junctions is secondary to vesicular transport. Colloidal carbon (a_e > 150 Å) does not penetrate the endothelium of uninjured capillaries. After injury, it appears to penetrate widened intercellular clefts between endothelial cells in venules and to be present in macropinocytotic vesicles of endothelial cells in venules and capillaries.[27, 28]

FENESTRATED CAPILLARIES

Tracer electron micrograph studies of capillaries of rat and mouse intestinal mucosa showed early concentrations of horse radish peroxidase, ferritin, and of dextrans and glycogens (a_e = 25–120 Å) outside a large fraction of the fenestrae.[18, 29] There was no correlation between the appearance of tracer and the presence or absence of a diaphragm. These tracers also were present in cytoplasmic vesicles in thicker parts of the cell, but transit appeared to be slower than through the fenestrae. Little or no tracer was found in the narrow part of the intercellular junctions.

These observations point to roles for membrane-lined vesicles, intercellular junctions, and fenestrae in transport of large molecules (a_e = 10 Å and larger), but do not identify other routes of transit available to water and small molecules. To evaluate the contribution of other pathways to material transport, we shall have to rely on data from kinetic studies of permeability.

The Cell Membrane Pathway

Cell membrane permeability has been characterized in terms of a lipid bilayer perforated by small pores with radii of 4 to as much as 10 Å.[30] This is certainly too simple a view, but it accounts for the observed magnitude of membrane permeability to water, for the comparatively high permeability to lipid-soluble substances and to very small nonpolar hydrophilic substances, and for the rapid reduction of cell permeability with increasing size for lipid-insoluble substances. If we assume "typical" permeability characteristics for capillary endothelial cell membranes, we are led to expect the cells to function as a passive transport pathway for water, small nonpolar solutes, and lipid-soluble solutes.

DIFFUSION OF WATER AND LIPID-SOLUBLE SOLUTES

According to Fick's law for a thin membrane, the rate of diffusion transport (mols/time) = PS ΔC, where P is the permeability coefficient, S the surface area, and ΔC the solute concentration difference. Permeability for diffusion exchange of water (P_w) has been shown to be high for capillaries in many organs by the use of tracers for water. However, water exchange in most organs is flow limited, and numerical values for comparison with water

permeabilities of cells have been obtained for only two organs, lung and brain, which may represent low extremes of diffusion permeability to water: dog lung,[31] $P_w = 4.4 \times 10^{-5}$ cm sec^{-1}; dog brain,[32] $P_w = 3.2 \times 10^{-5}$ cm sec^{-1}; monkey brain,[33] $P_w = 9.6 \times 10^{-5}$ cm sec^{-1}. These were all reported as PS products per unit organ weight from which P was obtained by dividing by the capillary surface area, S = 240 cm^2/g, an estimate which may be too small for the monkey brain. P_w for mammalian erythrocyte membranes is approximately 6×10^{-3} cm sec^{-1}, and for mammalian leukocytes, 1×10^{-4} cm sec^{-1}.[34] Allowing for two layers of membrane in series (the resistance of the cytoplasmic layer is 3 orders of magnitude less), we estimate through-the-cell permeability to be 5×10^{-5} to 3×10^{-3} cm sec^{-1}. The values for lung and brain capillaries lie close to the lower figure. High permeability of capillary walls to lipid-soluble substances has also been demonstrated[35, 36] and is thought to be an important factor in permitting rapid diffusion exchange of respiratory and anesthetic gases.[2] Capillary permeability to small, nonpolar, lipid-insoluble substances like urea is comparatively low, however, and it has been supposed that urea penetrates mainly by intercellular pathways.[37]

HYDRAULIC CONDUCTIVITY AND PERMEABILITY TO SMALL LIPID-INSOLUBLE SOLUTES

Table 1 illustrates the range of documented hydraulic conductivities (Lp) for different capillary types. Hydraulic conductivity is defined as the rate of volume flow (vol/time) per unit surface area and per unit hydrostatic or osmotic pressure difference. A more extensive table is given by Renkin and Curry.[1] Values of Lp for animal cell membranes lie mostly between 5×10^{-13} cm^3 sec^{-1} dyne^{-1} (mammalian leukocytes) and 2×10^{-11} cm^3 sec^{-1} dyne^{-1} (mammalian erythrocytes).[34] Allowing for two layers of membrane with a relatively nonresistant layer of cytoplasm between, we may imagine Lp for a tightly joined sheet of cells as falling between half these values. For the capillaries of rabbit brain, nearly all the hydraulic conductivity of water might be accounted for by the cell membrane path. Both P_W and Lp values for brain capillaries support the notion that intercellular pathways contribute little to transport. For the other nonfenestrated capillaries, as little as 2% or as much as 30% of the total Lp might be ascribed to the cell pathway, but in all cases intercellular pathways appear to be of substantial importance.

TABLE 1 *Hydraulic Conductivity of Capillary Endothelium*

	Lp (cm^3 sec^{-1} dyne^{-1})
Fenestrated capillaries	
1. Renal glomerulus (frog, mammal)	1.5×10^{-8}
2. Intestinal mucosa (mammal)	1.3×10^{-9}
Nonfenestrated	
3. Frog mesentery, rabbit omentum	5.0×10^{-10}
4. Rabbit heart	8.6×10^{-11}
5. Dog lung	3.4×10^{-11}
6. Cat hind leg	2.5×10^{-11}
Tight junction	
7. Rabbit brain	3.0×10^{-13}

Fenestrated capillaries display a still higher order of hydraulic conductivity, presumably due to complete dominance of transport pathways which do not transverse cell membranes. In capillaries with such high Lp, it is possible that the basement membrane or even the interstitial matrix contributes substantially to the overall resistance to fluid movement.[38]

Curry et al.[39] estimated the partition of hydraulic conductivity between cell membrane and extracellular pathways in capillaries of the frog's mesentery from measurements of the osmotic reflection coefficients (σ) of a series of small lipid-insoluble solutes graded with respect to molecular size. The osmotic reflection coefficient of a membrane for a specific solute is defined as the ratio of its observed osmotic effect to that predicted by van't Hoff's law: $\Delta C\ RT$, where ΔC is the solute concentration difference, R the gas constant, and T the absolute temperature. For a single membrane channel permeable to water, or a homogeneous population of channels, extrapolation of a plot of solute σ's to the molecular size of water (a_e = 1.5 Å) must yield a value of zero. The observed intercept was 0.10. On the assumption that the cell membrane was permeable to water, but not to any of the test solutes ($\sigma = 1$), they interpreted this to mean that 10% of the total volume flow passed through the cells and 90% by extracellular pathways. Since the surface area of the cells comprises more than 99% of the total endothelial surface, it may be estimated that Lp for the endothelial cell pathway is one-tenth of the value listed for these capillaries in Table 1, or 5×10^{-11} cm^3 sec^{-1} dyne^{-1}. This is still rather high compared to other cell membranes. Lp for the intercellular pathway is 4.5×10^{-10} cm^3 sec^{-1} dyne^{-1} (the area base being the entire capillary surface).

Several attempts have been made to fit single pathway models to the data of Pappenheimer et al.[37] for the capillaries of the cat's leg. These data consist of a series of measurements of P/σ for lipid-insoluble molecules graded with respect to molecular size. (At the time of their publication, the significance of Staverman's correction to van't Hoff's law was not generally known, and these values were believed to represent P; i.e., σ was taken to be one.) However, no single pathway model has been successful, i.e., internally consistent with respect to both σ and P as functions of molecular size.[1] Perl[40] tried to fit a two-pathway model to the data. He based the model on morphological data, which led him to specify intercellular slits 200 Å wide with a 40 Å restriction extending one-fifth their depth. By assigning 15% of total LpS to the cell membrane pathway ($\sigma = 1$) and 85% to the intercellular channels, he was able to get reasonable agreement between P's and σ's, though not uniformly over the full range of test molecule sizes.[41] Renkin and Curry[1] used an approach less dependent on specific geometric assumptions and obtained 10% for the fraction of Lp attributable to the cell membrane pathway and an equivalent pore radius for the intercellular channel of 50 Å. A fractional hydraulic conductivity for the cell pathway of 10–15% appears consistent with our previous comparison of capillary and cell membrane permeabilities for capillaries of this class. If the σ's for either model are used to calculate solute permeabilities, values are obtained

which are not only consistent with restricted diffusion theory, but which are very close to the values measured in human limbs by the indicator dilution methods.[42] (See below, and Table 2.)

Reflection coefficients for small lipid-insoluble molecules have also been reported for capillaries of rabbit heart[43] and dog lung.[44, 45] The heart data are consistent with a 10–90% division of Lp through cell membrane and extracellular channels, though the interpretation of Johnson et al. is a distributed population of pores, the smaller of which may represent cell membrane channels.[46] The two sets of data for dog lung are mutually incompatible, one suggesting an entirely extracellular porous pathway for water and small, lipid-insoluble solutes, the other a cell membrane pathway accounting for one-fourth to one-third of total hydraulic conductivity. Reflection coefficients for brain capillaries[47] are much higher than in other capillaries and approach unity for glucose and sucrose. This is consistent with the notion that the principal transport pathway is through the cells. The values for smaller molecules, e.g., urea, are lower than have been reported for some cell membranes, which may indicate the presence of a narrow intercellular pathway. The fall of σ with increasing a_e is reasonably consistent with a pore radius of 7 Å which is within the range of pore sizes attributed to cell membranes.[30] If brain capillaries are representative of the cell membrane pathway of capillaries in other organs, it is evident that these cells are not impermeable to urea, as we have assumed. On the other hand, Casley-Smith's observations of ferrocyanide and sulfate deposition suggests that a very narrow intercellular pathway may be present.[23]

Extracellular Pathways

Hydraulic conductivity in excess of that attributable to endothelial cells and permeability to lipid-insoluble molecules larger than urea are generally attributed to pathways which do not traverse cell membranes; morphological studies suggest intercellular junctions, fenestrae, or chains of fused vesicles opening to both cell surfaces. At least some of these channels are open to particles up to 100 Å or more in radius. Micropinocytotic vesicles are large enough to transport particles up to 250 Å radius. Interchange of single vesicles between the two endothelial surfaces would contribute to exchange of water and solutes but not to hydraulic conductivity.

PATHWAYS FOR LIPID-INSOLUBLE MOLECULES

Further characterization of extracellular pathways has been attempted by analysis of measured permeabilities to specific substances of known properties. Table 2 presents a compilation of measured permeabilities for lipid-insoluble molecules of graded sizes. Cerebral, nonfenestrated, and fenestrated capillaries are represented. The procedures used to obtain these data may be classified under

TABLE 2 *Capillary Permeability in Selected Organs to Graded Lipid-Insoluble Molecules of Moderate Size*

Substance	MW (g/mol)	D_{37} ($cm^2\ sec^{-1} \times 10^5$)	a_e* (Å)	P cm $sec^{-1} \times 10^6$ ($cm^3\ sec^{-1}$ per cm^2 capillary surface)								
				Cat leg P/σ (1)	Same, recalc (2)	Human forearm (3)	Dog gastric wall (4)	Sheep lung (term fetus) (5)	Dog lung (adult) (6)	Rabbit heart (7)	Dog heart (8)	Dog brain (9)
Na^+, Cl^- NaCl		1.8	2.3	314	34	36	77		4.7	64	>36	
Urea	60	1.9	2.6	234	26	28		4.1	6.0		27	4.6
Glycerol	92	1.2									13.4	2.1
Hexose†	180	0.91	3.6	91	10.7	13.1	33	0.42			9.3	1.6
Sucrose	342	0.72	4.7	50	6.1	8.6		0.39		18	7.1	0.2
Raffinose	504	0.58	5.7	39	5.4	5.3						
Inulin	5.5×10^3	0.22	15	6	1.4	0.9		0.11		2.0	2.3	
Myoglobin	17×10^3	0.17	19	0.6	0.3							
Serum albumin	69×10^3	0.09	35.5	0.01	0.01			0.06‡			0.03‡	<0.0001‡
S (capillary surface) $cm^2/100\ g \times 10^{-3}$§				7.0	7.0	7.0	12.5	90	300	56	56	24

MW = molecular weight, D_{37} = free diffusion coefficient (in water) at 37°, a_e = effective hydrodynamic radius (Stokes-Einstein).

All values of P were computed from experimental estimates of PS by dividing by the appropriate value of S. Data: (1) Pappenheimer et al.,[37] see also Landis and Pappenheimer.[2] PS/σ was obtained by simultaneous measurement of effective solute osmotic pressure and solute diffusion rate. In the original publication $\sigma = 1$ was assumed; therefore, these are maximal estimates. (2) Renkin and Curry.[1] Estimates of σ were made assuming 10% total hydraulic conductivity was through the cells ($\sigma = 1$ for all solutes), and 90% was through 50 Å radius pores (σ a function of a_e/r). (3) Trap-Jensen and Lassen.[42] PS was calculated from solute clearance ratios to a flow-limited reference (^{133}Xe) in exercise-vasodilated muscles at high blood flow rates. (4) Yudilevich et al.[50] Single-injection, multiple tracer method. (5) Normand et al.[51] Calculated from observed transport rates on the assumption of diffusion-limitation. The entry for hexose is mannitol. (6) Multiple tracer dilution at high flow. Na^+: Perl et al.,[36] Yipintsol.[52] Lung weight assumed 240 g. (7) Grabowski.[53] Multiple tracer dilution at high flow. (8) Alvarez and Yudilevich.[49] Multiple tracer dilution at high flow. (9) Crone.[54] The entry for hexose is fructose. Glucose transport in brain capillaries is carrier mediated.

* Stokes-Einstein radius, except for smallest molecules.[2]

† Hexose = glucose unless otherwise indicated.

‡ Transferred from Table 4, where origins are cited.

§ Sources of information about capillary surface area (S): (1, 2, 3) Pappenheimer et al.,[37] denervated, resting skeletal muscle. Not all capillaries are open. Casley-Smith et al.[55] give 3 times this figure for total capillary surface. (4) Casley-Smith et al.[38] dog jejunal wall, muscularis 40%, mucosa 60% of total S. (5, 6) Normand et al.,[51] Weibel.[56] (7, 8) Vargas and Johnson,[57] Bassingthwaite et al.[58] (9) Crone;[47] Weiderhold et al.[59] have recently reported a higher estimate, $65 \times 10^3\ cm^2/100\ g$.

two headings: (1) simultaneous measurement of transient osmotic effects and diffusion fluxes of test solutes introduced in substantial concentration in plasma[37, 43] and (2) direct measurement of diffusion rates at known blood flow, using trace concentrations of the test solute to avoid osmotic effects.[48, 49] Both approaches present serious practical and theoretical problems which remain only partly resolved. The specific method by which each column of data was obtained is indicated in the footnotes to the table. In all cases, the data was obtained originally as permeability-surface area products (PS) and then divided by a suitable estimate of capillary surface (S) in the organ studied to obtain permeability (P).[48]

Solute P declines with increasing a_e, due partly to the fall of free diffusibility and partly to steric restriction in the extracellular channels. The first two columns of data represent alternate interpretations of the relation of P to a_e for mammalian skeletal muscle, based on osmotic transient data. The first column gives the values originally obtained by Pappenheimer et al.[37] These are really P/σ, and are equal to P only if $\sigma = 1$ for all test molecules. They represent, therefore, the upper limits of P for each solute. Column 2 lists the P's calculated from these values on the assumption[1] of a two-pathway model with 10% Lp assigned to a cell membrane for which $\sigma = 1$ and 90% to an extracellular pore pathway of radius 50 Å. Column 3 lists P values measured for exercise-vasodilated human skeletal muscle by an isotope diffusion method.[42] These are remarkably close to the figures in column 2.

Pappenheimer has noted (personal communication) that the values of P for glucose in columns 2 and 3 of Table 2 are too small to account for glucose supply to exercising skeletal muscles by diffusion. According to Fick's law, $M = PS\Delta C$, where M = the steady state rate of transport and ΔC the concentration difference required. If we take M to be approximately 1 μM sec^{-1}/100 g,[60] $P = 12 \times 10^{-6}$ cm sec^{-1} and $S = 7 \times 10^3$ cm^2/100 g, it follows that ΔC glucose must be 12 μM ml^{-1} (mM/liter). Arterial glucose concentration is only 5 mM/liter, clearly insufficient for supply. Even if we allow for a 2.5-fold increase in S during exercise vasodilation in cat or dog skeletal muscle,[61] a concentration difference of 4.8 mM/liter would be required and this scarcely allows a margin of safety. The possibility of significant carrier transport or active transport of glucose across capillary walls is very small, since $P_{glucose}$ is not above the curve relating P to a_e for other lipid-insoluble substances. It is possible that glucose uptake by exercising skeletal muscle is limited by capillary permeability. However, it seems also possible that the values of P listed in columns 2 and 3 are underestimates of the true permeabilities.

Permeabilities for capillaries of rabbit and dog heart are fairly close to those for cat leg and human forearm, in conformity with the similar reflection coefficients and with the morphological similarity of capillaries in skeletal and cardiac muscle. The higher transport capacity (PS) of the microvascular bed in cardiac muscle for this class of solute, as well as its higher filtration coefficient (LpS) appears to be due to its greater capillary density.[62] For brain capillaries, permeabilities are much smaller than for capillaries in skeletal and cardiac muscle, and decrease more steeply with increasing molecular size. Glucose and certain amino acids are transported by chemically specific carriers.[54, 63] The tabulated data may be too high by almost an order of magnitude. Yudilevich and De Rose[63] were not able to measure statistically significant arteriovenous differences for Na^+, Cl^-, Rb^+, urea, glycerol, mannitol, or sucrose. Patlack and Fenstermacher[32] estimated P_{urea} in dog brain to be only 0.6×10^{-6} cm sec^{-1}, and stated that P's for larger solutes were even smaller. If these figures represent typical permeabilities of endothelial cells, then from 2% to 17% of the urea flux through capillaries of skeletal and cardiac muscle might go through the cell membrane pathway. It is a surprise to observe that lung capillaries, both in full-term fetal lambs and adult dogs (Table 2, columns 5 and 6), have permeabilities to small, lipid-insoluble molecules an order of magnitude less than muscle capillaries and not much larger than brain capillaries. The morphology of the pulmonary capillary endothelium is very like that of heart and skeletal muscle,[56] and its Lp is also similar (Table 1). For the fetal lamb lung, a low level of permeability extends to larger molecules than for the brain, to inulin and even serum albumin, with relatively little progressive restriction. These observations suggest that the "small pore" extracellular pathway is poorly developed in these capillaries and that much of the Lp is attributable to a well developed "large pore" pathway (see below).

The sole representation of fenestrated capillaries in Table 2 is the gastric wall of the dog. Only the mucosal capillaries are fenestrated, but if the proportions are the same as in jejunum, mucosal capillaries account for almost 60% of the total capillary surface per gram, and any increase in permeability above the level of the nonfenestrated capillaries in the muscularis should be observable. The entry in the first line is $^{38}Cl^-$ rather than NaCl or tracer Na^+, and it is not certain whether the high value of P is due to the greater mobility of Cl^- compared to Na^+, or to a 2-fold increase in the overall level of permeability. The high P for glucose is more significant. It is roughly 3 times $P_{glucose}$ for capillaries of cardiac or skeletal muscle. Assuming the 40% of total capillary surface in the muscularis smooth muscle to have the same $P_{glucose}$ as in skeletal muscle, $P_{glucose}$ for mucosal capillaries would be about 48×10^{-6} cm sec^{-1}, 4- to 5-fold greater. From this extremely limited data base, namely a 4- to 5-fold higher $P_{glucose}$ and a 20-fold higher Lp (Table 1), it appears that capillary fenestrations are associated with elevation of permeability to water and small molecules.

LARGE MOLECULES

In all capillary endothelia, a low level of permeability extends beyond the molecular size range covered by Table 2, above the size of hypothetical slit or pore models of the intercellular transport system for smaller molecules.[3] The steep fall of P with increasing a_e is limited by an extension of smaller slope, which may represent a separate transport mechanism, quantitatively insignificant for small molecules, but important for large. Grotte[64] identified this pathway with a few large "leaks" through the endothelium; Renkin[13] suggested that part or all of the extension of permeability beyond the small pore limit might be

TABLE 3 *Permeability of Capillaries in Selected Organs to dextran (D) or Polyvinylpyrrolidone (PVP) According to Molecular Size*

	P cm sec^{-1} × 10^8 (cm^3 sec^{-1} per cm^2)					
(Å) *	Dog paw (1)	Dog paw (2)	Rat cremaster muscle (3)	Dog intestine (4)	Sheep lung (5)	Dog heart (6)
18			127			
20			92			
22	34.7		68		10.1	
24	40.5				7.6	
28	24.4	29.9	26.7	25.9	5.0	
32	6.3				3.5	
36		8.1	10.6	6.6	2.9	
40		3.9		2.9		
46	3.0	1.7	5.2	1.0	1.8	2.7
52	2.2	1.0		0.5		0.7
60	2.0	0.5	2.8	0.3	1.1	0.3
70	1.2				0.8	0.4
80	0.4		1.1		0.6	0.4
90	0.4				0.5	0.4
110	0.9				0.4	0.3
	S cm^2/100 g × 10^{-3}†					
	7	7	7	12.5	90	56

(1) Garlick and Renkin;[65] PS = LR/(1-R). (2) Arturson and Granath.[68] Calculated as above, assuming L = 5.7 × 10^{-4} ml/sec × 100 g. (3) Youlten[69] PVP. The exposed cremaster in situ was superfused with Ringer's solution, and the amount transported into the superfusate measured. P for serum albumin = 5.4 × 10^{-8} cm sec^{-1}. (4) Arturson and Granath.[68] Calculated as in (1) with L assumed to be 3.5 × 10^{-4} ml/sec × 100 g.[70,71] (5) Boyd et al[72] PVP. Calculated as in (1) from L and R. (6) Areskog et al.[73] Calculated as in (1) from L and R.

* Values from various sources were normalized by linear interpolation. In most instances, a_e was determined by gel chromatography. Dextran unless otherwise indicated.

† See notes to Table 2 for sources of these figures.

attributed to transport by micropinocytotic vesicles (cytopempsis).

Tables 3 and 4 present summaries of data for macromolecular transport in selected organs, largely derived from studies of lymph flow and composition. The permeabilities listed in Tables 3 and 4 are diffusion permeabilities, calculated on the assumption that diffusion or vesicular exchange rather than convection is the dominant mode of transport in this size range.[13,65] To the extent that convective transport is involved, they are *overestimates* of the true permeabilities.[66,67] These values are probably adequate as approximations for comparison of capillaries of different organs. In any event, they will have to do, since evaluation of convective and diffusive components of large molecule transport is only beginning to be realized (see below).

The data for long-chain, flexible polymers (Table 3) present more or less continuous sequences of molecular size. For all organs, permeability falls progressively with increasing molecular size, with only minor and probably insignificant exceptions. Below a_e = 30 Å, the fall is steep; this represents the upper bound of "small pore" permeability. Above this level, the fall is more gradual, characteristic of the "large pore," "leak," or vesicular transport system. The data for plasma protein fractions (Table 4) form a less smoothly continuous series. The effects of molecular size on permeability are complicated by differences in charge and configuration. The range of molecular sizes represents mainly the "large pore" extension. For the same organ, capillary permeabilities to dextran or polyvinylpyrrolidone (PVP) and to proteins appear comparable for similar molecular sizes.

Protein permeabilities of brain capillaries are three orders of magnitude lower than for the other entries in Table 4. Even these figures are probably overestimates, since most of the protein leakage into cerebrospinal fluid probably takes place through the capillaries of the choroid plexus. For both paw capillaries and brain capillaries, permeability to transferrin is distinctly higher than to serum albumin, even though it is a slightly larger molecule. Carter et al.[74] attributed this effect in paw capillaries to the smaller negative charge on transferrin. Except for the cerebral capillaries, there are no really large differences in permeability to proteins or to polymers among

TABLE 4 *Permeability of Capillaries in Selected Organs to Plasma Proteins**

				P cm sec^{-1} × 10^8 (cm^3 sec^{-1} per cm^2)					
Substance	MW (g/mol × 10^{-3})	D_w, 37 (cm^2 sec^{-1} × 10^7)	a_e (Å)	Dog paw (1)	Dog intestine (2)	Sheep lung (fetus) (3)	Sheep lung (adult) (4)	Dog heart (5)	Human brain (6)
α-Globulin	45	11.0	30	5.7	2.8				0.008
Serum albumin	69	9.3	35.5	4.7	2.9	5.6	1.4	2.9	0.008
Transferrin	90	7.6	43	6.3					0.013
Haptoglobin[1-1]	100	7.2	46	3.1	1.4				
γ-Globulin	160	5.9	56	3.3		1.7	0.2	1.5	0.002
α_2-Macroglobulin	820	3.7	91		0.7	0.6			0.0004
Fibrinogen	340	3.1	108	1.6					
[S cm^2/100 g × 10^{-3}†				7	12.5	90	300	56	24.]

(1) Carter et al.[74] (2) Calculated from R data of Ganrot et al. (1969)[75] assuming L = 3.5 × 10^{-4} ml/sec × 100 g.[70,71] Intestine weight was taken as 6.5% body weight.[76] (3) Boyd et al.[72] (4) Calculated from data of Brigham et al.[77] (5) Calculated from data of Areskog et al.[73] (6) Dr. S. I. Rapoport (personal communication) calculated permeabilities by equation A, below, from the CSF protein data of Felgenhauer[78] and attributed them to the choroid plexuses, S = 14 cm^2/100 g brain. To obtain *maximal* estimates of protein permeabilities of cerebral capillaries, I have recalculated his figures on a total capillary surface basis (S = 24 × 10^3 cm^2/100 g brain). Since attribution of most protein leakage into cerebrospinal fluid to the choroid plexuses seems entirely reasonable, the actual P values for cerebral capillaries must be much less.

* Equation A: PS = LR/(1-R), calculated for normal levels of lymph flow, L. This formula neglects convective transport, and thus overestimates PS, particularly at high flows.[13,66,67]

† See notes to Table 2 for sources of these figures.

capillaries of the organs represented. All but intestinal capillaries are nonfenestrated. The polymer data for dog paw (two sets) and rat skeletal muscle (cremaster) are remarkably similar. Permeabilities of dog heart capillaries to proteins and to dextrans are slightly lower than dog paw capillaries. Permeabilities of fetal sheep lung capillaries are generally similar to those of dog heart, though serum albumin permeability is twice as great. The adult sheep lung shows distinctly lower permeabilities to plasma proteins.

Estimates of "large pore" radii for these capillaries, derived from the relation of permeability to molecular size, are in the range 300–1000 Å or more and their numbers are surmised to be much lower than those of the small pores.[2, 3, 64, 65, 73, 74] Accuracy of such estimates is limited by the narrow range of molecular sizes in most experiments and by difficulties of evaluating molecular size and in measuring transport rates of very large molecules. Structural features of these dimensions are well within the range of electron microscopic resolution, but the pores are few and far between, which must make it hard to distinguish reality from artifacts. Attempts currently being made to localize large molecule leaks with the light microscope before studying them by electron microscopy should be helpful in identifying their morphological counterparts.

It comes as a distinct surprise to find that the capillaries of dog intestine, the only representation of fenestrated capillaries in Tables 3 and 4, do not show a higher level of macromolecular permeability than the other, nonfenestrated capillaries (except for brain). It was noted above that for fenestrated capillaries of the gastric mucosa, permeability for small, lipid-insoluble molecules was higher. However, there is no indication that the presence of fenestrae is associated with increased permeability to macromolecules. If we accept the EM-tracer evidence that a large fraction of the fenestrae permit passage of particles as large as 100 Å radius,[18] we must conclude that the basement membrane or some other external structure limits the diffusion of such molecules. The morphological evidence is not clear on this point, in the case of either fenestrated or nonfestrated capillaries. Further studies on fenestrated capillaries by both approaches are needed to resolve this question.

CHANNELS VS. VESICULAR TURNOVER

Palade[11] and numerous others after him have suggested that a large part of macromolecular transport across capillary walls could be attributed to exchange of micropinocytotic vesicles between internal and external surfaces. The dynamic characteristics of this process are similar to diffusion, except that vesicles, rather than individual molecules, are the units supposed to move randomly through the membrane.[79, 80] It has been possible, using appropriate models of vesicular motion, to relate observed rates of solute transport to observed tracer transit times. Reasonable agreement has been obtained for molecules the size of serum albumin and larger; for small molecules, much shorter transit times are required than have been measured by particulate tracers.[65, 74] A further refinement of this analysis was introduced in the form of a theoretical relation for molecular exclusion from spherical vesicles.[65] This has permitted comparison of transport rates for molecules of different sizes, evaluation of a hypothetical vesicular radius, and calculation of the total volume of fluid turned over by this process. For capillaries of the dog paw, the decreasing exchange of dextrans and plasma proteins with increasing molecular size led to a predicted internal vesicular radius of 250 Å, which corresponds closely to the observed dimensions.

Since the kinetics of vesicular turnover cannot be distinguished from those of diffusion through open channels, partition of total transport for a given macromolecule into "large pore" and vesicular components from the values of P given in Tables 3 and 4 can only be arbitrary: such a number of pores if all transport is by pores, such a turnover rate of vesicles if all transport is by vesicles. The difference between vesicular and pore transport lies in the hydraulic conductivity of a continuous channel through the endothelium. In the presence of volume flow through such a channel, an additional flux of permeating solutes due to solvent drag is superimposed on the diffusion flux.[2, 67] Such an addition is not to be expected for vesicular turnover. Therefore, any experimental maneuver which can vary the rate of volume flow could be used to distinguish between the two processes or to apportion total permeation between the two. An attempt to do this for dog paw capillaries was made by Garlick and Renkin[65] who used venous congestion to elevate the volume flow. Their results were variable in individual trials: in some experiments solute flux was not increased, in others it was increased in proportion to the volume flow. It appeared as if, on the average, about half the transport of molecules larger than serum albumin could be assigned to large pores, half to large vesicles.

A more detailed study of the effect of volume flow on transport of macromolecules in the dog paw has been made by Renkin et al.[81, 82] Volume flow was increased by step-wise venous congestion. When venous pressure was held above 45 mm Hg for some time, signs of increased permeability to large molecules appeared (see Landis et al.[83]); the results described below exclude such data. With increasing lymph flow, lymph-plasma concentration ratios for plasma proteins and dextran (a_e = 70 Å) fell, but solute flux (flow × concentration ratio) increased.

Analysis according to the principles of irreversible thermodynamics and hydrodynamics[1, 67] permitted independent evaluation of P and σ from such data. The values of P obtained were about two-thirds of the values listed in Table 4. The reflection coefficients for these substances lay between 0.83 and 0.95. The relation of σ to a_e for plasma proteins suggested a restrictive porosity of 280 Å radius (or parallel-walled slit-width of 400 Å). Extrapolation of σ to the molecular radius of water yielded a value of 0.19 rather than zero, which indicates that 19% of total hydraulic conductivity can be attributed to this "large pore" pathway. If 10% is assigned to the cell membrane pathway, 71% of total Lp is left for the small pore pathway (radius, 40–50, Å).

Calculation of the number of large pores required to account for 19% of total hydraulic conductivity yields a figure of one per 5000 small pores (ratio of cross-sectional areas, 6×10^{-3}). The diffusion permeability of the large pores to plasma proteins according to this reckoning is only about one-fourth the actually observed values. The remaining three-fourths was attributed to vesicular turnover. The actual volume exchange was estimated to be 2×10^{-8} cm^3 sec^{-1} per cm^2 endothelial surface, which amounts to 3×10^8 vesicles of internal radius 250 Å per second. The total number of vesicles present[54] is about 10^{10}/cm^2.

Taylor et al.[84] used a similar approach to evaluate σ and PS for total plasma proteins in capillaries of several organs, including examples of both fenestrated and nonfenestrated endothelium. Their values of σ for serum albumin in dog leg capillaries are similar to those of Renkin et al., in intestine and and lung capillaries, somewhat lower. In all cases, σ tended to increase with increasing lymph flow. The latter observation suggests heteroporosity. However, until data are available for a range of molecular sizes, further characterization of the transport pathways is not possible.

Summary

Morphological and physiological studies indicate multiple routes for transport across capillary endothelium. However, the identification of the morphological counterparts of specific transport processes (or the assignment of specific transport roles to morphologically identifiable pathways) has been only partly achieved: the contribution of endothelial cell membranes to transport of water and small, lipid-insoluble molecules needs to be evaluated. The identification of the "small pore" pathway for water and lipid-insoluble molecules with the intercellular junctions still remains questionable. The contributions to total macromolecular transport of junctions, single vesicles (pinocytosis, cytopempsis), chains of vesicles, and fenestrae are not yet known.

References

1. Renkin EM, Curry FE: Transport of water and solutes across capillary endothelium. *In* Handbook of Epithelial Transport, edited by G Giebisch, DC Tosteson, 1978 (in press)
2. Landis EM, Pappenheimer JR: Exchange of substances through the capillary walls. *In* Handbook of Physiology, sect 2, Circulation, vol II, ch 29, edited by WF Hamilton, P Dow. Washington, D.C., American Physiological Society, 1963, pp 961-1034
3. Mayerson HS: The physiologic importance of lymph. *In* Handbook of Physiology, sect 2, Circulation, vol II, ch 30, edited by WF Hamilton, P Dow. Washington, D.C., American Physiological Society, 1963, pp 1035-1073
4. Majno G: Ultrastructure of the vascular membrane. *In* Handbook of Physiology, sect. 2, Circulation, vol III, ch 64, edited by WF Hamilton, P Dow. Washington, D.C., American Physiological Society, 1965, pp 2293-2375
5. Michel CC: Flows across the capillary wall. *In* Cardiovascular Fluid Dynamics, vol II, edited by DH Bergel. London, Academic Press, 1972, pp 241-298
6. Renkin EM, Gilmore JP: Glomerular filtration. *In* Handbook of Physiology, sect 8, ch 9, Renal Physiology, edited by J Orloff and RW Berliner. Washington, D.C., American Physiological Society, 1973, pp 185-248
7. Brenner BM, Bayliss C, Deen WM: Transport of molecules across renal glomerular capillaries. Physiol Rev **56:** 502-534, 1976
8. Bennett HS, Luft JH, Hampton JC: Morphological classification of vertebrate blood capillaries. Am J Physiol **196:** 381-390, 1959
9. Simionescu M, Simionescu N, Palade GE: Morphometric data on the endothelium of blood capillaries. J Cell Biol **60:** 128-152, 1974
10. Rhodin JAG: The diaphragm of capillary endothelial fenestrations. J Ultrastruct Res **6:** 171-185, 1962
11. Palade GE: Transport in quanta across the endothelium of blood capillaries (abstr). Anat Rec **116:** 254, 1960
12. Palade GE and Bruns RR: Structural modulations of plasmalemmal vesicles. J Cell Biol **37:** 633-649, 1968
13. Renkin, EM: Transport of large molecules across capillary walls. Physiologist **7:** 13-28, 1964
14. Scow RO, Blanchette-Mackie EJ and Smith LC: Role of capillary endothelium in the clearance of chylomycrons; a model for lipid transport from blood by lateral diffusion in cell membranes. Circ Res **39:** 149-162, 1976
15. Simionescu M, Simionescu N and Palade GE: Segmental differentiations of cell junctions in the vascular endothelium; the microvasculature. J Cell Biol **67:** 863-885, 1975
16. Schneeberger EE and Karnovsky MJ: Substructure of intercellular junctions in freeze-fractured alveolar capillary membranes of mouse lung. Circ Res **38:** 404-411, 1976
17. Simionescu N, Simionescu M and Palade, GE: Permeability of muscle capillaries to small heme-peptides; evidence for the existence of patent transendothelial channels. J Cell Biol **64:** 586-607, 1975
18. Simionescu N, Simionescu M and Palade GE: Permeability of intestinal capillaries; Pathway followed by dextrans and glycogens. J Cell Biol **53:** 365-392, 1972
19. Levick JR, Michel CC: The permeability of individual perfused frog mesenteric capillaries to T1824 and T1824-albumin as evidence for a large pore system. Q J Exp Physiol **58:** 67-85, 1973
20. Michel CC and Levick JR: Variations in permeability along individually perfused capillaries of the frog mesentery. Q J Exp Physiol **62:** 1-10, 1977
21. Nakamura Y and Wayland H: Macromolecular transport in the cat mesentery. Microvasc Res **9:** 1-21, 1975
22. Florey H: Capillary permeability (abstr). J Physiol **61:** i, 1925
23. Casley-Smith JR: An electron microscopical demonstration of the permeability of cerebral and retinal capillaries to ions. Experientia **25:** 845-847, 1969
24. Simionescu N, Simionescu M and Palade GE: Permeability of muscle capillaries to exogenous myoglobin. J Cell Biol **57:** 424-452, 1973
25. Karnovsky MJ: The ultrastructural basis of capillary permeability studied with peroxidase as a tracer. J Cell Biol **35:** 213-236, 1967
26. Bruns RR and Palade GE: Studies on blood capillaries. II. Transport of ferritin molecules across the wall of muscle capillaries. J Cell Biol **37:** 277-299, 1968
27. Marchesi VT: The passage of colloidal carbon through inflamed endothelium. Proc R Soc Lond [Biol] **156:** 550-552, 1962
28. Cotran RS, Suter ER and Majno G: The use of colloidal carbon as a tracer for vascular injury. Vasc Dis **4:** 107-127, 1967
29. Clementi F and GE Palade: Intestinal capillaries. I. Permeability to peroxidase and ferritin. J Cell Biol **41:** 33-58, 1969
30. Solomon AK: Characterization of biological membranes by equivalent pores. J Gen Physiol **51:** 335s-364s, 1968
31. Harris TR, Rowlett RD and Brigham KL: The identification of pulmonary capillary permeability from multiple-indicator data; effects of increased capillary pressure and alloxan treatment in the dog. Microvasc Res **12:** 177-196, 1976
32. Patlak CS, Fenstermacher JD: Measurements of dog blood-brain transfer constants by ventriculocisternal perfusion. Am J Physiol **299:** 877-884, 1975
33. Raichle ME, Eichling JO, Straatmann MG, Welch MJ, Larson KB and Ter-Pogogian MM: Blood brain barrier permeability of ^{11}C-labelled alcohols and ^{15}O-labelled water. Am J Physiol **230:** 543-552, 1976
34. House CR: Water Transport in Cells and Tissues. (monographs of the Physiological Society, edited by H Davson, ADM Greenfield, R Whittam, GS Brindley). London, Edward Arnold, 1974
35. Renkin EM: Capillary permeability to lipid-soluble molecules. Am J Physiol **168:** 538-545, 1952
36. Perl W, Silverman F, Delea AC and Chinard FP: Permeability of dog lung endothelium to sodium, diols, amides and water. Am J Physiol **230:** 1708-1721, 1976
37. Pappenheimer JR, Renkin EM and Borrero LM: Filtration, diffusion and molecular sieving through peripheral capillary membranes; a contribution to the pore theory of capillary permeability. Am J Physiol **167:** 13-46, 1951
38. Casley-Smith JR, O'Donoghue PJ and Crocker KWJ: The quantitative relation between fenestrae in jejunal capillaries and connective tissue channels; proof of "tunnel capillaries." Microvasc Res **9:** 78-100, 1975
39. Curry FE, Mason JC and Michel CC: Osmotic reflexion coefficients of capillary walls to low molecular weight hydrophilic solutes measured in single perfused capillaries of the frog mesentery. J Physiol (Lond) **261:** 319-336, 1976
40. Perl W: Modified filtration-permeability model of transcapillary trans-

port; a solution of the Pappenheimer pore puzzle? Microvasc Res **3:** 233–251, 1971
41. Curry FE: A hydrodynamic description of the osmotic reflection coefficient with application to the pore theory of transcapillary exchange. Microvasc Res **8:** 236–252, 1974
42. Trap-Jensen J, Lassen NA: Restricted diffusion in skeletal muscle capillaries in man. Am J Physiol **220:** 371–376, 1971
43. Vargas F and Johnson JA: An estimate of reflection coefficients from rabbit heart capillaries. J Gen Physiol **47:** 667–677, 1964
44. Taylor AE and Gaar KA Jr.: Estimation of equivalent pore radii of pulmonary capillary and alveolar membranes. Am J Physiol **218:** 1133–1140, 1970
45. Perl W, Chowdhury P and Chinard FP: Reflection coefficients of dog lung endothelium to small hydrophilic solutes. Am J Physiol **228:** 797–809, 1975
46. Johnson JA, Levitt DG, Wangensteen OD and Bloom G: A distributed pore size model for capillaries. Microvasc Res **10:** 217–219, 1975
47. Fenstermacher JD and Johnson JA: Filtration and reflection coefficients of the rabbit blood-brain barrier. Am J Physiol **211:** 341–346, 1966
48. Crone C: The permeability of capillaries in various organs as determined by use of the "indicator diffusion" method. Acta Physiol Scand **58:** 292–305, 1963
49. Alvarez OA and Yudilevich DL: Heart capillary permeability to lipid-insoluble molecules. J Physiol **202:** 45–58, 1969
50. Yudilevich DL, Renkin EM, Alvarez OA and Bravo I: Fractional extraction and transcapillary exchange during continuous and instantaneous tracer administration. Circ Res **33:** 325–336, 1968
51. Normand ICS, Olver RD, Reynolds EOR and Strang LB: Permeability of lung capillaries and alveoli to non-electrolytes in the foetal lamb (with an appendix by K. Welch). J Physiol **219:** 303–330, 1971
52. Yipintsoi T: Single-passage extraction and permeability estimation of sodium in normal dog lungs. Circ Res **39:** 523–531, 1976
53. Grabowski EF, Bassingthwaighte JB: An osmotic weight transient model for estimation of capillary parameters in myocardium. *In* Microcirculation, vol 2, Transport Mechanisms, Disease States, edited by J Grayson, W Zingg. New York, Plenum Press, 1976, pp. 29–50
54. Crone C: The permeability of brain capillaries to nonelectrolytes. Acta Physiol Scand **64:** 407–417, 1965
55. Casley-Smith JR, Green HS, Harris JL and Wadey PJ: The quantitative morphology of skeletal muscle capillaries in relation to permeability. Microvasc Res **10:** 43–64, 1975
56. Weibel ER: Morphological basis of alveolar-capillary gas exchange. Physiol Rev **53:** 419–495, 1973
57. Vargas F and Johnson JA: Permeability of rabbit heart capillaries to nonelectrolytes. Am J Physiol **213:** 87–93, 1967
58. Bassingthwaighte JB, Yipintsoi T and Harvey RB: Microvasculature of the dog left ventricular myocardium. Microvasc Res **7:** 229–249, 1974
59. Weiderhold KH, Bielser W Jr., Schulz U, Veteau MJ and Hunziker O: Three-dimensional reconstruction of brain capillaries from frozen serial sections. Microvasc Res **11:** 175–180, 1976
60. Chapler CK and Stainsby WN: Carbohydrate metabolism in contracting dog skeletal muscle in situ. Am J Physiol **215:** 995–1004, 1968
61. Renkin EM, Hudlická O and Sheehan RM: Influence of metabolic vasodilatation on blood-tissue diffusion in skeletal muscle. Am J Physiol **211:** 87–98, 1966
62. Renkin EM: Blood flow and transcapillary exchange in skeletal and cardiac muscle. *In* Coronary Circulation and Energetics of the Myocardium edited by G Marchetti, B Taccardi. Basel, S Karger, 1967, pp 18–30
63. Yudilevich DL and De Rose N: Blood-brain transfer of glucose and other molecules measured by rapid indicator dilution. Am J Physiol **220:** 841–846, 1971
64. Grotte G: Passage of dextran molecules across the blood-lymph barrier. Acta Chir Scand Suppl **211:** 1–84, 1956
65. Garlick DG and Renkin EM: Transport of large molecules from plasma to interstitial fluid and lymph in dogs. Am J Physiol **219:** 1595–1605, 1970
66. Schultze HE and Heremans JR: Molecular Biology of Human Proteins (with Special Reference to Plasma Proteins). Nature and Metabolism of Extracellular Proteins. vol 1. Amsterdam, Elsevier 1966
67. Perl W: Convection and permeation of albumin between plasma and interstitium. Microvasc Res **10:** 83–94, 1975
68. Arturson G and Granath K: Dextrans as test molecules in studies of the functional ultrastructure of biological membranes. Clin Chim Acta **37:** 309–322, 1972
69. Youlten LJF: The permeability to human serum albumin and polyvinylpyrrolidone of skeletal muscle (rat cremaster) blood vessel walls. J Physiol **204:** 112–113P, 1969
70. Nix JT, Mann FC, Bollman JL, Grindlay JH and Flock EV: Alterations of protein constituents of lymph by specific injury to the liver. Am J Physiol **164:** 119–122, 1951
71. Johnson PC and Richardson DR: The influence of venous pressure on filtration forces in the intestine. Microvasc Res **7:** 296–306, 1974
72. Boyd RDH, Hill JR, Humphreys PW, Normand ICS, Reynolds EOR and Strang LB: Permeability of lung capillaries to macromolecules in foetal and newborn lambs and sheep. J Physiol **201:** 567–588, 1969
73. Areskog NH, Arturson G, Grotte G and Wallenius G: Studies on heart lymph II. Capillary permeability of the dog's heart using dextran as a test substance. Acta Physiol Scand **62:** 218–233, 1964
74. Carter RD, Joyner WL and Renkin EM: Effect of histamine and some other substances on molecular selectivity of the capillary wall to plasma proteins and dextran. Microvasc Res **7:** 31–48, 1974
75. Ganrot PO, Laurell CB and Ohlsson K: Concentration of trypsin inhibitors of different molecular size and of albumin and haptoglobin in blood and lymph of various organs in the dog. Acta Physiol Scand **79:** 280–286, 1970
76. Skelton H: The storage of water by various tissues of the body. Arch Int Med **40:** 140–152, 1927
77. Brigham KL, Woolverton WC, Blake LH and Staub NC: Increased *sheep lung vascular permeability caused by pseudomonas bacteremia*. J Clin Invest **54:** 792–804, 1974
78. Felgenhauer K: Protein size and cerebrospinal fluid composition. Klin. Wochenschr **52:** 1158–1164, 1974
79. Tomlin SG: Vesicular transport across endothelial cells. Biochem Biophys Acta **183:** 559–564, 1969
80. Shea SM, Karnovsky MJ and Bossert WH: Vesicle transport across endothelium; simulation of a diffusion model. J Theor Biol **24:** 30–42, 1969
81. Renkin EM, Joyner WL, Sloop CH and Watson PD: Influence of venous pressure on plasma-lymph transport in the dog's paw. Convective and dissipative mechanisms. Microvasc Res **14:** 191–204, 1977
82. Renkin EM, Watson PD, Sloop CH, Joyner WL, Curry FE: Transport pathways for fluid and large molecules in microvascular endothelium of the dog's paw. Microvasc Res **14:** 205–214, 1977
83. Landis EM, Jonas L, Angevine M and Erb W: The passage of fluid and protein through the human capillary wall during venous congestion. J Clin Invest **11:** 717–734, 1932
84. Taylor AE, Granger DN and Brace RA: Analysis of lymphatic protein flux data. I. Estimation of the reflection coefficient and *permeability surface area product for total protein*. Microvasc Res **13:** 297–313, 1977